Physical and chemical modified forms of palm shell: Preparation, characterization and preliminary assessment as adsorbents

ARTICLE *in* JOURNAL OF POROUS MATERIALS · FEBRUARY 2012

Impact Factor: 1.11 · DOI: 10.1007/s10934-012-9571-4

3 AUTHORS, INCLUDING:

Shilpi Kushwaha
CSIR - National Chemical Laboratory, Pune
25 PUBLICATIONS **133** CITATIONS
SEE PROFILE

P. Padmaja
The Maharaja Sayajirao University of Baroda
36 PUBLICATIONS **215** CITATIONS
SEE PROFILE

J Porous Mater
DOI 10.1007/s10934-012-9571-4

Physical and chemical modified forms of palm shell: preparation, characterization and preliminary assessment as adsorbents

S. Kushwaha · G. Sreelatha · P. Padmaja

Abstract A series of adsorbents were obtained from palm shell (*Borassus flabellifer*) powder (PSP) which is an agro-waste. PSP was carbonized using sulphuric acid (APSP). APSP was subjected to the following modification procedures: activation to different temperatures (3AAC, 6AAC, 7AAC and 9AAC); activation with steam and persulfate (SAPSP and PAPSP) at 140 °C. Further the effect of modification of PSP, APSP, SAPSP and PAPSP using formaldehyde (MPSP, MAPSP, MSAPSP and MPAPSP) was also investigated. The materials were characterized using SEM, FTIR, TGA and XRD. N_2 adsorption isotherms, DR equation and BJH methods were used to characterize the pore structure of the prepared carbons. The iodine value for APSP, SAPSP and PAPSP were found to be 342.5, 199.8, 299.7 mg/g respectively. They were also found to have large pores as well as chelating functional groups indicating their potential adsorption capacity. The carbon 9AAC was found to have high BET surface area of 834 m^2/g and a pore volume of 0.4474 cm^3/g with predominant micro-pores. Selectivity coefficients for different mixtures containing mercury, copper, zinc and cadmium have been determined for PSP, MPSP, APSP, SAPSP, PAPSP and 9AAC. Though PSP, APSP, SAPSP, PAPSP and MPSP did not have appreciable surface area, they showed encouraging results for adsorption of heavy metals indicating the potential use of palm shell as an economic precursor in the activated carbon preparation process.

Keywords *Borassus flabellifer* · Palm shell powder · Agro-waste · Modification · Heavy metals

1 Introduction

Activated carbon is well known as an efficient adsorbent because of its porosity and large surface area. It has thus been widely used in the sorption of gases and chemical species from aqueous solution. However, commercial activated carbon is expensive and thus alternative cost effective activated carbon is the need of the day. Cost effective activated carbons can be prepared from a variety of raw materials. Some of the most commonly used precursors are agro-wastes like nutshells, fruit stones, rice bran and rice husk due to ecological and economic significance [1–4].

Generally activated carbons are produced by carbonizing the raw material prior to activation. Carbonization is necessary to increase the carbon content and for the development of porous material. The pores are further developed by activation. Mesoporous activated carbons are applied in liquid phase adsorption while micro-porous activated carbons are used for the adsorption of gases and vapors. The adsorption capacity of activated carbons from aqueous solutions is largely controlled by their surface characteristics. There are several critical parameters affecting the production of activated carbons with specific surface properties. Carbonization temperature affects the shapes of pores in the carbon. High temperature char samples have higher micro-pore volume [5, 6]. To prepare

Electronic supplementary material The online version of this article (doi:10.1007/s10934-012-9571-4) contains supplementary material, which is available to authorized users.

S. Kushwaha · P. Padmaja (✉)
Department of Chemistry, Faculty of Science, The Maharaja Sayajirao University of Baroda, Vadodara, India
e-mail: p_padmaja2001@yahoo.com

G. Sreelatha
Department of Applied Chemistry, Faculty of Technology and Engineering, The Maharaja Sayajirao University of Baroda, Vadodara, India

Published online: 01 March 2012

mesoporous carbons activation to high burn off degrees, physical and chemical activation [7–12], catalytic activation in the presence of transition metals [13, 14] and template carbonization [15–18] have been used.

Presently, low cost forest and agricultural wastes with or without little processing are considered promising adsorbents for heavy metals due to their high surface area, micro-porous character and surface chemical nature [8]. Besides, they are cheaper and readily available materials. Coconut shell, nutshells, oil palm waste, pine needles, sawdust, waste straw, rice husk, peanut hulls, hazelnut shells, almond shells, peach stones, tea dust leaves, apple wastes, sugarcane bagasse, coffee grounds, banana and orange peels, sugar beet pulp and various other materials have been investigated [19–27].

The objective of this work was to study the effects of acid treatment with H_2SO_4, followed by other activation techniques on the surface area, porosity and surface chemistry of lingo-cellulosic material. Outer shell of palm fruit (*Borassus flabellifer*) is a cheap and abundant agricultural by-product in tropical countries. Hence the feasibility of the use of palm shell powder (PSP) as a precursor for the preparation of different adsorbents by charring using H_2SO_4 (APSP) at 140 °C, steam treatment of APSP (SAPSP), persulfate treatment of APSP (PAPSP), activation to higher temperatures of APSP (3AAC, 6AAC, 7AAC and 9AAC) and formaldehyde treatment of PSP, APSP, SAPSP and PAPSP (MPSP, MAPSP, MSAPSP and MPAPSP) have been explored. The textural characterization and adsorption potential of the prepared adsorbents have been studied. Parallel to these studies our group had also observed that APSP displayed great potential for different types of dyes [28] and pesticides [29]. Encouraged with the results and looking into the abundant functional groups present in PSP, MPSP, APSP, SAPSP, PAPSP, as well as the high surface area of 9AAC, preliminary studies on the adsorption ability of these adsorbents towards heavy metals like Cu, Cd, Zn and Hg was also done for binary, ternary and quaternary metal systems. In waste waters usually single pollutant is not present. Competitive adsorption on the adsorbent surface can take place where components with similar properties (i.e., size, polarity, interaction energy) compete for a limited number of adsorption sites. Thus, a better understanding of the multicomponent adsorption from aqueous solutions is needed.

2 Materials and methods

2.1 Preparation of *Borassus flabellifer* (PSP) based adsorbents

The shells of palm fruit (*B. flabellifer*) were collected from coastal Andhra Pradesh, India, and were cut into small pieces. The pieces were extensively washed with running tap water for 30–40 min to remove dirt and other particulate matter followed by double distilled water. The pieces were dried in an oven at 70 °C, ground in a laboratory blender and sorted using standard test sieves. The sample used was of particle size passing 40 μ sieve and is henceforth termed as PSP.

The PSP was modified by using different techniques (Scheme 1). PSP was treated with conc. H_2SO_4 in a ratio of 1:1.5 wt/volume with continuous stirring. The charred substance was then heated in an air oven at 140 °C for 24 h. The sample was then extensively washed with a solution of 2% $NaHCO_3$ until the effervescence ceased, and further kept in 2% $NaHCO_3$ overnight. After washing with distilled water 2–3 times, the sample was then kept in an air oven for 4 h at 105 °C. The prepared acid treated PSP is termed as APSP.

APSP was modified by different methods—(1) APSP was treated with steam in an electric autoclave for 30 min at 14 psi pressure and the product obtained was termed as SAPSP. (2) PAPSP was obtained by treating APSP with conc. H_2SO_4 in the ratio of 1:1.5 wt/volume in presence of 0.1% $K_2S_2O_8$ and was kept in an air oven for 4 h at 140 °C. Subsequently it was washed extensively with 2% $NaHCO_3$ until effervescence ceased and left overnight soaked in 2% $NaHCO_3$. Finally it was washed 2–3 times with distilled water and then again dried in an air oven at 105 °C for 4 h.

Modification of PSP, APSP, SAPSP and PAPSP with formaldehyde was done in order to polymerize and immobilize the color and water soluble substances. One gram each of PSP, APSP, SAPSP and PAPSP were soaked in 100 mL of 0.2% formaldehyde solution for 24 h. The resulting MPSP, MAPSP, MSAPSP and MPAPSP were then filtered, washed with 300 mL of distilled water several times, and dried overnight in an oven at 60 °C.

To see the effect of temperature on surface area of APSP, thermal activation was done at four different temperatures 300 °C (3AAC), 600 °C (6AAC), 700 °C (7AAC), 900 °C (9AAC). The heating was carried out with a programmable muffle furnace at a rate of 50°C/min until the desired temperatures were reached and then kept at that temperature for 1 h. The samples 3AAC, 6AAC, 7AAC and 9AAC were then washed with 2% $NaHCO_3$ until effervescence ceased, and were left soaked in 2% $NaHCO_3$ overnight. Finally they were washed 2–3 times with distilled water and then again dried in an air oven at 105 °C for 4 h.

2.2 Characterization techniques and methods of analysis

Physical properties (bulk density, moisture content, solubility in water and acid) and chemical properties (pH, ion

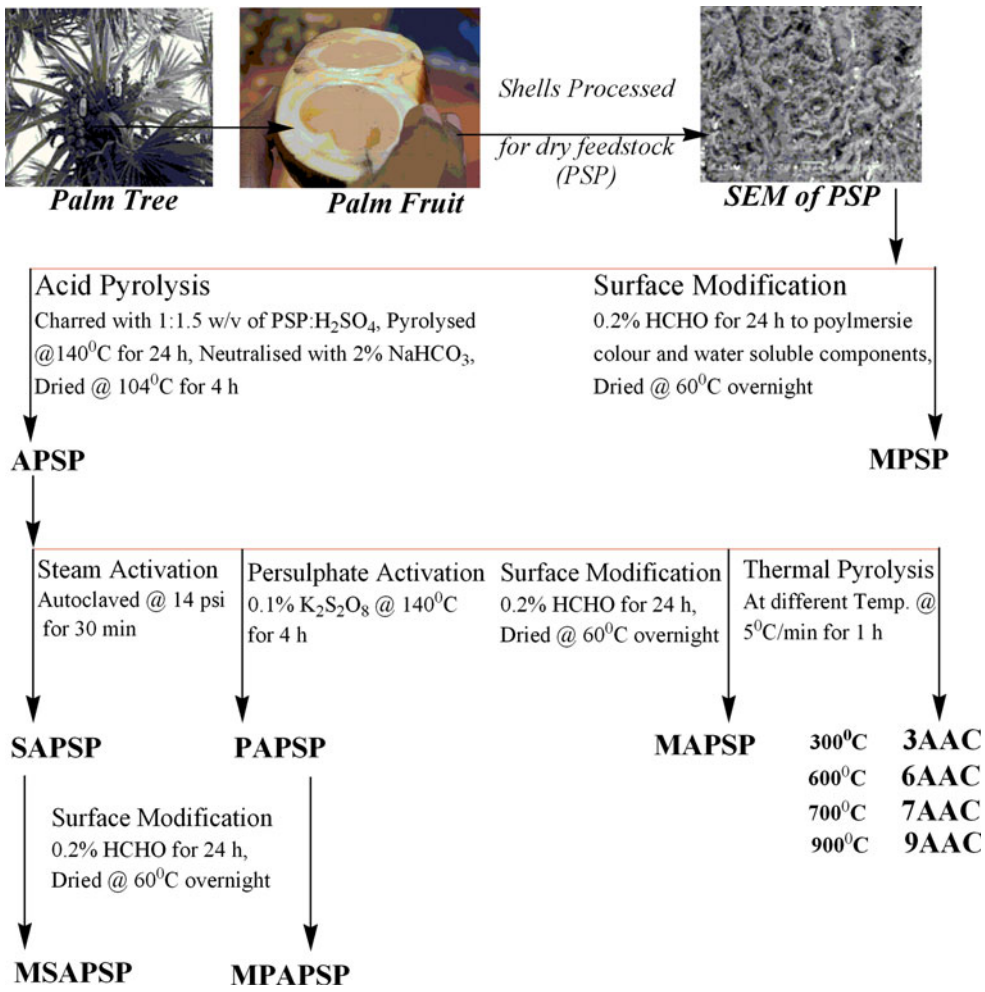

Scheme 1 Different methods of modification of palm shell powder

exchange capacity) of the prepared adsorbents were investigated. Bulk density measurements were done using a previously weighed 100 mL graduated cylinder and filling it up to 50 mL mark with the adsorbent under study. The cylinder with the carbon was weighed accurately. The apparent density was calculated by dividing the difference in weight by 50. Moisture content was found out by heating a known weight of the sample in an air oven maintained at 105 ± 5 °C for about 4 h. Heating, cooling and weighing were repeated at 30 min time interval till the difference between two consecutive weighings was less than 5 mg. Solubility in water and acid was determined by taking ten gram of adsorbent under study into a 1 L beaker and boiling with 300 mL distilled water and 0.25N HCl respectively followed by digestion for around 30 min. The material was washed thoroughly with distilled water and washings were collected along with the filtrate. The filtrate was concentrated on a water bath, cooled and made up to 100 mL in a volumetric flask. Exactly 50 mL of the concentrate was transferred to a china dish, evaporated to almost dryness on a water bath and finally dried in an electric oven maintained at 105 ± 5 °C, cooled and weighed. The weight of the residue represents the matter soluble in water and acid. The pH was measured by heating a suspension of ten gram adsorbent in 300 mL distilled water to boiling with constant stirring. The solution was then digested for around 30 min. The material was filtered, cooled and pH of the solution was measured. For measuring the ion exchange capacity, 0.5 g of adsorbent under study was added to 100 mL solution of 0.25 M sodium sulphate in a stoppered conical flask and kept for shaking in a temperature controlled shaking bath for 5 h. The contents were filtered and the filtrate was titrated against 0.1N NaOH using phenolphthalein indicator. The ion exchange capacity of the adsorbent in meq/g was calculated from the following equation.

$$\text{Ion exchange capacity}\left(\frac{\text{meq}}{\text{g}}\right) = \frac{aW}{V}$$

where a = normality of NaOH, V = volume of NaOH, W = weight of the adsorbent in g.

Iodine value was calculated by means of adsorption of iodine from aqueous solution which can be used to compare adsorbent surface areas and is a relative indicator of

porosity [30]. A sample of 0.2 g of adsorbent under study was equilibrated with iodine/iodide solution and the iodine residual concentration was determined by titrating with sodium thiosulphate solution.

Iodine value = (blank − burette reading for sample) × conversion factor, mg/g.

$$\text{Conversion factor} = \frac{\text{Mol. wt. of iodine}(127) \times 40}{\text{Wt. of carbon} \times \text{blank reading}}$$

Blank reading: Burette reading for iodine concentration without adding the carbon sample. Burette reading for sample: Burette reading for iodine remaining unadsorbed in solution after adding the carbon sample.

The iodine number is a relative indicator of porosity in a carbonaceous material and may be used as an approximation of surface area for some types of carbons [30]. Correlation between the BET surface area and the iodine number is established and well documented [4, 31, 32]. As iodine number gives an indication on micro-porosity (pores less than 1 nm in diameter), higher iodine numbers reflect better development of the micro-porous structure and higher adsorption abilities for low-molar-mass solutes [31, 33, 34].

All the experiments were carried out in triplicate and the average results are given. The thermal behavior of the adsorbents was evaluated by using thermo-gravimetric analyzer (TG–DTA 32, SEIKO Thermal Analysis System SS 5100), under air at a heating rate of 10 °C/min^{-1}. Adsorption characteristics of the adsorbents were determined by nitrogen adsorption at 77.37 K (Surface Area Analyser Micromeritics, ASAP 2020 V3.03H). The specific surface areas were determined from the isotherms using the Brunauer–Emmett–Teller equation. The *t*-plot and DR plot methods were applied to calculate the pore volume and the BJH method was used for pore size distribution determination [3, 35]. The surface morphology and topographic analysis of the adsorbent samples was examined by scanning electron microscope (JEOL, Model JSM-5610LV). Samples were mounted onto metal holders using a conducting substrate. Powder-XRD of the ingredients was taken by holding the samples in place on quartz plate for exposure to CuKα radiation of wavelength 1.5406 Å. The sample was analyzed at room temperature over a range of 10–70° 2θ with sampling intervals of 0.02° 2θ and scanning rate of 60/min. Fourier Transform Infra Red spectra were collected by a Perkin Elmer RX1 model within the wave number range of 400–4,000/cm. Specimens of samples were first mixed with KBr and then ground in an agate mortar at an appropriate ratio of 1/100 for the preparation of the pellets. Resulting mixture was pressed at 10 tons for 5 min sixteen scans and 8/cm resolution were applied in recording spectra. The background obtained from the scan of pure KBr was automatically subtracted from the sample spectra.

The adsorption ability of the adsorbents under study (PSP, MPSP, APSP, SAPSP, PAPSP and 9AAC) for Cu, Cd, Zn and Hg in binary, ternary and quaternary metal solution mixtures was investigated. Binary mixtures contained 25 ppm of each metal ion, ternary mixtures contained 11 ppm of each metal ion and quaternary mixtures contained 6.25 ppm of each metal ion. Batch experiments were performed by taking 20 mL of adsorbate solution containing different mixtures of metal ions under study maintained at pH 4 and 0.1 g of adsorbent in 25 mL stoppered flasks. The contents were shaken by a thermostated water bath shaker with a constant speed of 150 rpm at 30 °C and the samples were withdrawn at appropriate time intervals and filtered. The filtrate was analyzed for each of the metals Cu, Cd, Zn and Hg by AAS at their respective wavelengths.

3 Result and discussion

3.1 Physical characterization of adsorbents

The series of adsorbents namely APSP, SAPSP, PAPSP, MAPSP, MSAPSP, MPAPSP, 3AAC, 6AAC, 7AAC and 9AAC prepared from PSP by different routes and different activating agents were characterized for various characteristics like bulk density, solubility in water, solubility in acid, ash content, moisture content and ion exchange capacity and are tabulated in Table 1.

It can be observed from the table that bulk density of activated carbons in each case is higher than PSP. Moisture content was in the range of 2.6–19.1%. The moisture content detected was due to the contact of moisture from atmosphere after activation. Solubility in water and acid is negligible for PSP, MPSP, 3AAC, 6AAC, 7AAC and 9AAC. All the adsorbents prepared have pH in the range (6.0–8.0) which is appropriate for water treatment purpose. APSP, SAPSP, PAPSP, 3AAC have a pH of ~7.5–8.0 while the others have a neutral to near neutral pH of 6.0–7.1. pH values of the adsorbents under study are lower than reported pH values of commercial activated carbons. Ion exchange capacity is significantly increased and was found to be the highest for MPSP (0.5) followed by MAPSP and 6AAC (0.25), 7AAC and 9AAC (0.167), APSP (0.125) and SAPSP (0.110). The other modified forms had comparatively low ion exchange capacity.

Adsorbents that can remove a high percentage of iodine normally have a high surface area and also largely a micro- and meso-porous structure [36]. It can be seen from the Figure S1 that on modification with formaldehyde the iodine value was higher (312.41 mg/g) as compared to PSP (146.82 mg/g) but was slightly lower to that of APSP (342.47 mg/g). Temperature variation from 300 to 900 °C

Table 1 Physical characterization of adsorbents

Sample	Bulk density (gm/cm^3)	Moisture content (%)	pH	Solubility in H_2O (%)	Solubility in acid (%)	Ion exchange capacity (meq/gm)	Ash content (%)
PS	0.3516	8.372	6.0	3.44	4.04	0.0041	0.897
APSP	0.5502	2.6	8.05	12.33	15.61	0.125	6.653
SAPSP	0.5768	14.58	7.75	53.4	51.2	0.110	6.893
PAPSP	0.6262	16.34	8.0	25.3	27.7	0.0714	6.783
MPSP	0.362	9.343936	7.10	2.5	3.91	0.5	1.098
MAPSP	0.553	15.32338	6.80	10.0	13.06	0.25	5.47
MSAPSP	0.5788	19.14257	6.41	36.5	38.10	0.124	5.23
MPAPSP	0.5518	17.62376	6.32	6.0	8.1	0.125	6.98
3AAC	0.6484	11.5653	7.6	3.5	4.2	0.0139	1.409
6AAC	0.5494	9.327984	6.99	3.5	4.71	0.25	4.678
7AAC	0.4488	9.081836	6.95	0.0	0.04	0.167	9.532
9AAC	0.5398	15.9	6.90	0.5	0.92	0.167	10.989

during thermal activation of APSP resulted in an increase in iodine value from 436.82 to 990.44 mg/g which is comparable with reported values.

3.2 Thermal characterization of adsorbents

Thermal analysis curves (DTG, DTA and TGA) are shown (Figure S2). The weight loss during thermo-gravimetric decomposition of the adsorbents can be divided into different stages and tabulated in Table 2. The TGA curves of the adsorbents showed a first stage weight loss of 4–16% in the region below 145 °C corresponding to the loss of water molecules. The second stage (145 °C $< T <$ 600 °C), which corresponds to the primary carbonization, is seen as a large weight loss (36–95%) for the adsorbents suggesting the elimination of volatile matters and tars. Above 600 °C, SAPSP, PAPSP, MAPSP, MPAPSP and 3AAC showed very little weight loss (1–10%) indicating their decomposition to a structure with higher stability while APSP and MAPSP showed a higher weight loss of 20–32%, indicating that more surface functional groups are created on APSP and MAPSP [37]. The TGA curves indicate that thermal stability is greater for 9AAC. Gergova [38] and Krisztina [39] have also reported three stages in the carbonization process and the formation of basic structure at 800–900 °C in lingo-cellulosic materials.

3.3 BET surface area measurements/N_2 adsorption isotherms

Adsorption isotherms of nitrogen for the adsorbents are shown in Figure S3. N_2 uptake was found to be very less in

Table 2 Thermal analysis

Sample name	Weight loss (%)							
	1st Stage	Temperature range (°C)	2nd Stage	Temperature range (°C)	3rd Stage	Temperature range (°C)	4th Stage	Temperature range (°C)
PSP	5.61	26.1–99.9	89.21	207.3–493.7	–	–	1.91	493.7–858.3
APSP	10.48	30.5–99.9	36	99.9–478.0	8.2	478.0–746.4	31.6	746.4–829.2
SAPSP	13.9	28.3–124.5	–	–	38.59	124.5–750.9	33.54	750.9–858.3
PAPSP	14.57	30.5–129.0	61.71	129.0–578.7	1.92	578.7–748.7	9.6	748.7–860.5
MPSP	6.059	30.5–205.1	90.5	205.1–495.9	–	–	2.1	495.9–858.3
MAPSP	16.596	30.6–135.7	54.6	135.7–585.4	–	–	19.9	585.4–860.6
MSAPSP	11.04	26.1–102.2	–	–	40.08	102.2–717.4	33.29	717.4–858.3
MPAPSP	15.199	30.5–144.6	62.5	144.6–558.5	–	–	10.1	708.4–858.3
3AAC	12.745	28.3–135.7	83.6	135.7–486.9	–	–	1.3	486.9–858.3
6AAC	7.147	30.6–102.1	2.1	102.1–305.7	86.1	305.7–560.8	–	–
7AAC	4.56	30.5–95.4	33.5	95.4–372.8	80	372.8–547.3	–	–
9AAC	4.326	32.8–84.3	4.25	84.3–406.4	80.4	406.4–623.4	–	–

PSP, APSP, SAPSP, PAPSP, MPSP, MAPSP, MSAPSP, MPAPSP and 3AAC. The shapes of the isotherms are different as a result of different porosities. The porosities seem to be same for MPSP, MAPSP, MSAPSP and 3AAC and similar for APSP, PSP and PAPSP. Predominant adsorption finishes at a very low relative pressure and the amount of nitrogen adsorbed decreased for 3AAC, MAPSP, MPSP, PSP indicating that pore cavities are micro-porous/blocked. The nitrogen adsorption isotherms of 9AAC, 7AAC and 6AAC show increase in amount of nitrogen adsorbed with relative pressure which reflect a certain amount of meso-pore volume. It is observed that the carbons 6AAC and 7AAC exhibit type II isotherms, indicating an indefinite multi-layer formation after completion of the monolayer and is found in adsorbents with a wide distribution of pore sizes. Near to the first point of inflexion a monolayer is completed, following which adsorption occurs in successive layers, while 9AAC exhibits type IV adsorption curve with a hysteresis loop (in the relative pressure range of 0.8–1), which is associated with capillary condensation in meso-pores. The hysteresis loops are different in 6AAC, 7AAC suggesting the presence of pores with different shapes. The nitrogen adsorption isotherm of 9AAC shows a tremendous increase in N_2 uptake compared to 6AAC and 7AAC. The adsorption was found to be higher at low relative pressure for 6AAC, 7AAC and 9AAC suggesting the presence of relatively larger number of micro-pores. Type III isotherm is obtained for 3AAC which occurs when affinity between adsorbent and adsorbate is less than adsorbate–adsorbate interactions. BET isotherm is not applicable for calculation of surface area in such adsorbents.

PSP, APSP, SAPSP, PAPSP, MPSP, MAPSP, MSAPSP, MPAPSP show type I isotherm according to BET classification indicating monolayer adsorption and are typical of micro-porous samples and hence not amenable to BET analysis [40]. BET surface area measured for different activated carbons is presented in Table 3. The carbons APSP, SAPSP, PAPSP, MAPSP, MSAPSP and MPAPSP do not show high BET surface area but adsorption property as seen by iodine value is higher. They may contain a number of narrow micropores inaccessible (within reasonable time) to N_2 at 77 K [41]. The iodine number is considered as a simple method to evaluate the surface area of activated carbons associated with pores with $d > 1$ nm. The carbons prepared at higher carbonization temperatures (6AAC, 7AAC and 9AAC) have significantly increased pore volume (0.218, 0.23 and 0.447 cm^3/g) and BET surface area (469, 476 and 835 m^2/g); with supportive evidence from Iodine values. BET surface area is higher than BJH surface area, which agrees well with observations made by Gregg and Sough [42]. Till 700 °C the temperature was not high enough to achieve the complete decomposition of PSP. Thus the low surface area of 3AAC, 6AAC and 7AAC are due to the presence of non decomposed or partially decomposed products in the pores of the carbon. On heating to 900 °C the decomposition of these products was also complete and pores were liberated and surface area increased to 846 m^2/g. BET surface area is highest for 9AAC forming mainly micro-pores. A comparison has been made for the surface area of different activated carbons and presented in Table 6. It is evident that the surface area of 9AAC is comparable to that of other activated carbons prepared from agro-wastes reported in literature.

3.3.1 Pore structure and pore size distribution

The extent of the micro-porosity and the development of the pore structure under different conditions used were

Table 3 Surface area analysis

Adsorbent unit	Single point SA (m^2/g)	BET SA (m^2/g)	Langmuir SA (m^2/g)	BJH pore SA (m^2/g)	BJH pore volume (cm^3/g)	BET av. pore dia. (Å)
PSP	0.6	0.7	1.0	–	0.00401	237.984
APSP	0.2	0.3	0.4	–	0.00315	422.652
SAPSP	2.1	2.4	3.9	–	0.00491	81.2444
PAPSP	0.1	0.1	0.1	–	0.02232	9,829.99
MPSP	0.4	0.5	0.7	–	0.00379	301.04
MAPSP	0.3	0.3	0.4	–	0.00158	201.73
MSAPSP	2.8	3.4	6.3	–	0.00547	64.24
MPAPSP	0.1	0.2	0.2	–	0.00107	243.823
3AAC	0.3	0.1	0.1	–	0.00119	–
6AAC	470	469	597	50	0.21799	18.5688
7AAC	477	476	607	80	0.2303	19.3486
9AAC	846	834	1,083	163	0.4474	21.436

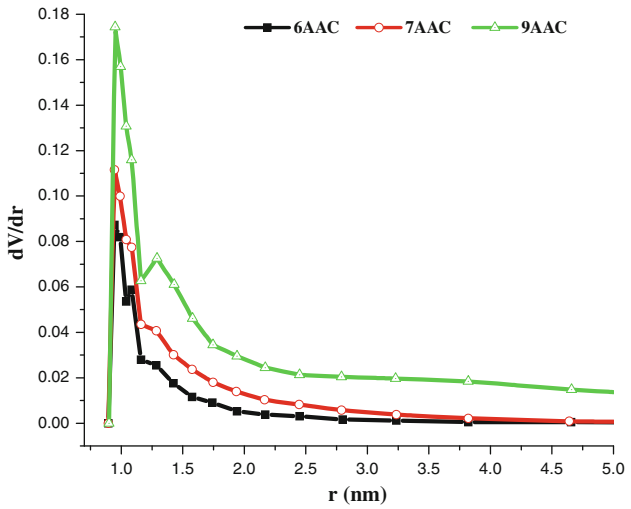

Fig. 1 Pore size distribution graph

evaluated by identifying the micro and meso-pore volumes and pore size distributions presented in Fig. 1.

Micro-pore volumes were analyzed by DR and *t*-plots as shown in Table 4. The *t*-plot [16] estimates the pore volume by assuming that layers build up on the wall of the pores until the pore is completely filled. The DR method [43] describes the adsorption according to the mechanism of volume filling. It can be seen from Table 4 that the *t*-plot slightly underestimates the micro-pore volume showing values lower than those from DR. This feature is probably due to the high values of the surface area. Remy and Poncelet [44] suggested that the DR equation overestimated $W_{0,DR}$, with respect to $W_{0,t}$, when a solid presents an high surface area. The micro-pore volumes determined from the DR plot (Fig. 2) increase with increase in temperature of APSP.

For 6AAC, 7AAC and 9AAC DR plots exhibited a brief linear range and then they deviate upward indicating formation of multilayer and capillary condensation in the meso-pores. Furthermore the meso-pores (2–50 nm) increased with increase in temperature of activation i.e. increasing the extent of burn off (6AAC, 7AAC and 9AAC) as a consequence of enhanced pore formation and pore widening effect. Micro-pore volumes for 6AAC, 7AAC and 9AAC are in the range of 0.18–0.30 which is comparable to those reported in literature [3]. Thus increase of carbonization temperature resulted in creation of micro-pore structure and widening of micro-pores to meso-pores and an increase in the total pore volume of carbons as seen in Table 3. Similar observations were made by Adinata et al. and Ismadji and Bhatia [45–47].

The pores of the carbons 6AAC, 7AAC and 9AAC are mostly located in the range of micropores with a peak at 1.2 nm. It is seen from the Tables 3 and 4 that BET surface area as well as micropore volume were highest for 9AAC suggesting that micro-pores make the largest contribution to the surface area. At high carbonization temperatures more ordered structure is likely to be developed in the carbon that leads to a lower rate of gasification in the interior of the particles [48]. Thus activated carbon high in micro-porosity is produced. PSP, APSP, SAPSP, PAPSP showed small BET surface area and small pore volume suggesting the entry of the gas molecules was partially restricted.

The value of E_0 provides a first indication for the presence or absence of micro-porosity in carbons. Typical micro-pores correspond to $E_0 > 18$–20 kJ/mol (APSP, PAPSP, 6AAC, 7AAC and 9AAC), whereas values below 14–15 kJ/mol reflect either variable degrees of surface heterogeneity, or the presence of super-micro-pores (1.5–2.5 nm) [49].

Table 4 Constants from DR plot for the adsorbents

Adsorbent unit	E (kJ/mol)	E_0 (kJ/mol)	W_0 (cm^3/g)	Micropore volume (*t*-plot) (cm^3/g)	Mesopore volume (cm^3/g)
PSP	4.227	12.432	0.000518	–	–
APSP	6.456	18.988	0.000342	–	–
SAPSP	1.456	4.2823	0.00195	–	–
PAPSP	6.1534	18.097	0.000187	–	–
MPSP	4.5672	13.432	0.000421	–	–
MAPSP	4.6544	13.689	0.00028	–	–
MSAPSP	5.489	16.144	0.000318	–	–
MPAPSP	2.872	8.1976	0.001455	–	–
3AAC	0.906	2.665	0.0000005	–	–
6AAC	11.0702	32.559	0.21387	0.178998	0.038992
7AAC	9.0277	26.55	0.22088	0.16805	0.06225
9AAC	7.9255	23.309	0.39874	0.2957	0.1517

Gas volumes were multiplied by 0.001547 to get liquid volumes

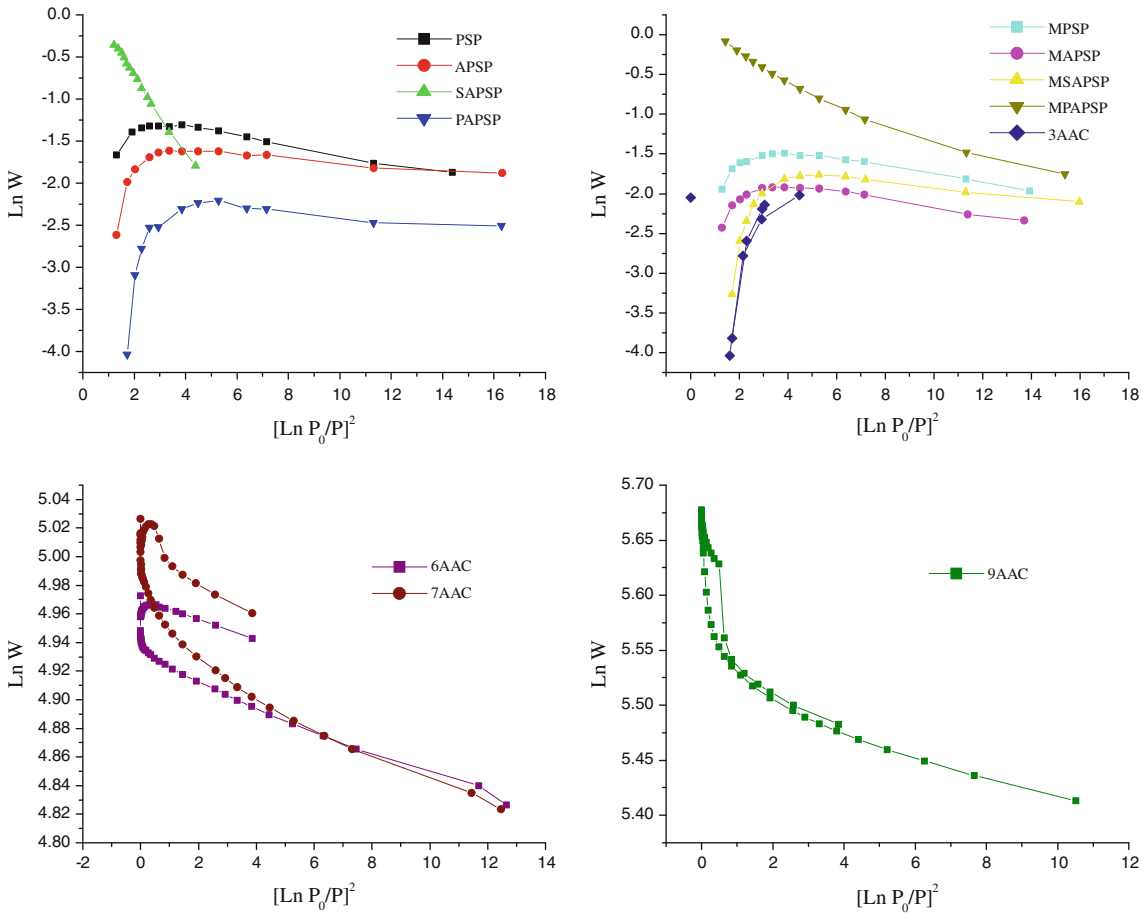

Fig. 2 DR plot for the adsorbents

3.4 Scanning electron micrographs

The micrograph in Fig. 3 shows the surface morphologies of PSP and the prepared adsorbents. The activated and modified adsorbents are having large particle size which is developed like a coral shell. A channel of tubes passing through can be observed. Cross section of some particles has been taken showing distorted pores. Porosity can be seen but not homogeneous, and some pores are broken also which may not support adsorption, in SAPSP and MSAPSP. The pores are superficial and bulk of the sample does not seem to have any porosity, resulting in less surface area.

In 6AAC, 7AAC and 9AAC defined surface porosity is seen to develop with temperature. Bulk porosity distributed in an even manner can be observed in some of the cross sections suggesting possible higher adsorption capacity as supported by iodine number and BET surface area parameters.

3.5 X-ray diffraction studies of carbons

The X-ray diffraction patterns of PSP and the other adsorbents under study are presented in Fig. 4 with the major peaks and their respective 2θ values tabulated in Table S1. XRD shows no characteristic peaks after activation at higher temperature. (6AAC, 7AAC and 9AAC) suggesting turbostratic structure of disordered carbon materials. There is a broad peak at 2θ value of 25° for all the materials under study. Sharp non-labelled peaks in PSP, APSP, SAPSP, PAPSP, and MPSP show miscellaneous inorganic components. Peak spacings of PSP and APSP at 0.430 and 0.281 nm are assigned to hkl 200 and 004 crystallographic planes of completely ordered regions of cellulose respectively, if a monoclinic unit cell is assumed with C as the fiber axis [50]. It is observed that in MSAPSP, MPAPSP the strong peaks are progressively losing intensity and becoming broader indicating a gradual decrease in cellulose crystallinity. A complete loss of crystal structure in cellulose is indicated by disappearance of 0.160 nm signals and shift of ~0.420 nm signal to higher angles in 3AAC, 6AAC, 7AAC and 9AAC. Similar observations were reported by Marco [51] during activation at different temperatures.

Peak spacings at ~0.60, ~0.53 nm in MPSP and PSP can be assigned to 101, 110 crystallographic planes of cellulose. Increased intensity of the 101 and 100 planes

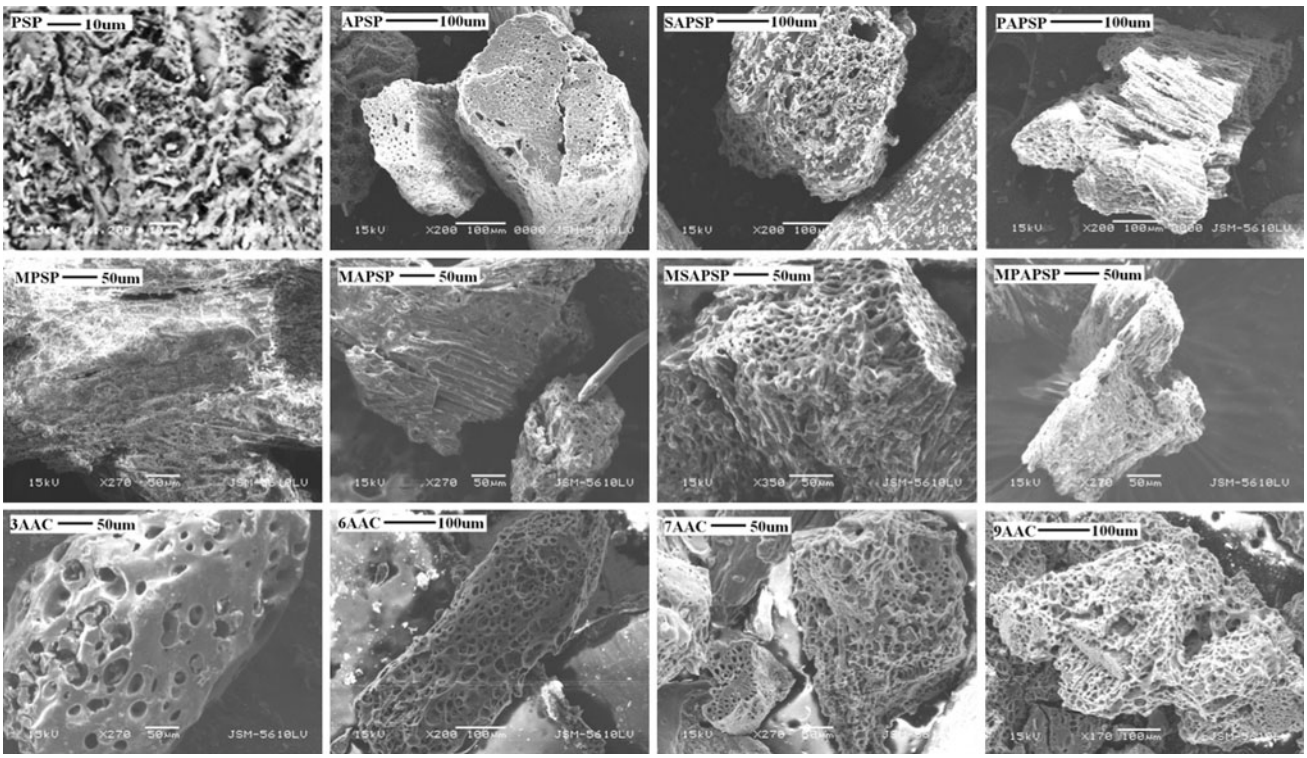

Fig. 3 Scanning electron micrographs

at 0.220 nm in MPSP indicates lateral growth of graphene planes. Broadening of XRD signal with increasing temperature at ~0.37 nm (23°) in 7AAC suggests the dominance of small aromatic units arranged in random order which may be attributed to the (002) reflection of a graphitic-type lattice. A weak reflection centered around 43° corresponds to a superposition of the (100) and (101) reflections of a graphitic-type carbon structure, indicating a limited degree of graphitization in this material [52]. Narrowing of peak ~0.4 nm with increasing temperature indicates developing atomic order in 9AAC and is attributed to the formation of turbostatic crystallites, i.e. progressive stacking of graphene sheets [53, 54].

3.6 Functional group analysis using FTIR

The possible modifications in the functional groups of palm shell upon charring and activation were studied by infrared spectroscopy (Table 5; Figure S4).

The presence of absorption bands characteristic of $–CH_3$ or $–CH_2$ symmetric stretching vibrations in the spectra of all the adsorbents suggests the existence of some aliphatic species on all the adsorbents under study. For PSP, APSP, PAPSP and SAPSP the bands in the frequency range 1,723–1,732 cm^{-1} indicate the presence of carboxylic acid groups as shown in Table 5. On charring with sulphuric acid (APSP) a new band at 1,770 cm^{-1} appears which is characteristic of carbonyl moieties in carboxylic anhydrides [55–63]. The band at ~1,348–1,373 cm^{-1} for the adsorbents under study corresponds to vibrations in alkanes and alkyl groups, whereas the band near 1,589–1,597 cm^{-1} is attributed to aromatic ring stretching coupled to highly conjugated carbonyl groups. The presence of bands at 1,101–1,180 cm^{-1} in 3AAC, PSP and MPSP can be attributed to stretching frequency of the bonds in ester, ether and the phenol groups. 1,348–1,373 cm^{-1} is the characteristic peak of carbohydrates seen in PSP, APSP, SAPSP, PAPSP and MPSP. After formaldehyde treatment there seems to be a slight change in morphology probably due to the reaction of hydroxyl groups of cellulose with formaldehyde which is indicated by the absence of bands in the frequency range 1,723–1,732 cm^{-1} [63]. The bands at 1,079.82, 835.91 cm^{-1} are characteristic of carbohydrate units [64]. The bands for 3AAC at 1,592 cm^{-1}, MPSP at 1,512 and 1,387 cm^{-1}, MSAPSP at 1,578 and 1,375 cm^{-1} and APSP at 1,378 cm^{-1} suggests that lignin present in palm shell is still not completely depolymerised. The presence of bands at 1,725 cm^{-1} in the case of PAPSP, and at 1,734 cm^{-1} in PSP and MPSP is indicative of –C=O stretching of aromatic esters, aldehydes, ketones and acetyl derivatives. Cyclic compounds containing conjugated C=C and C=N may be responsible for the absorption bands observed at 846–809 cm^{-1} except for SAPSP [55–57]. Absorption band in the region 666–750 cm^{-1} can be

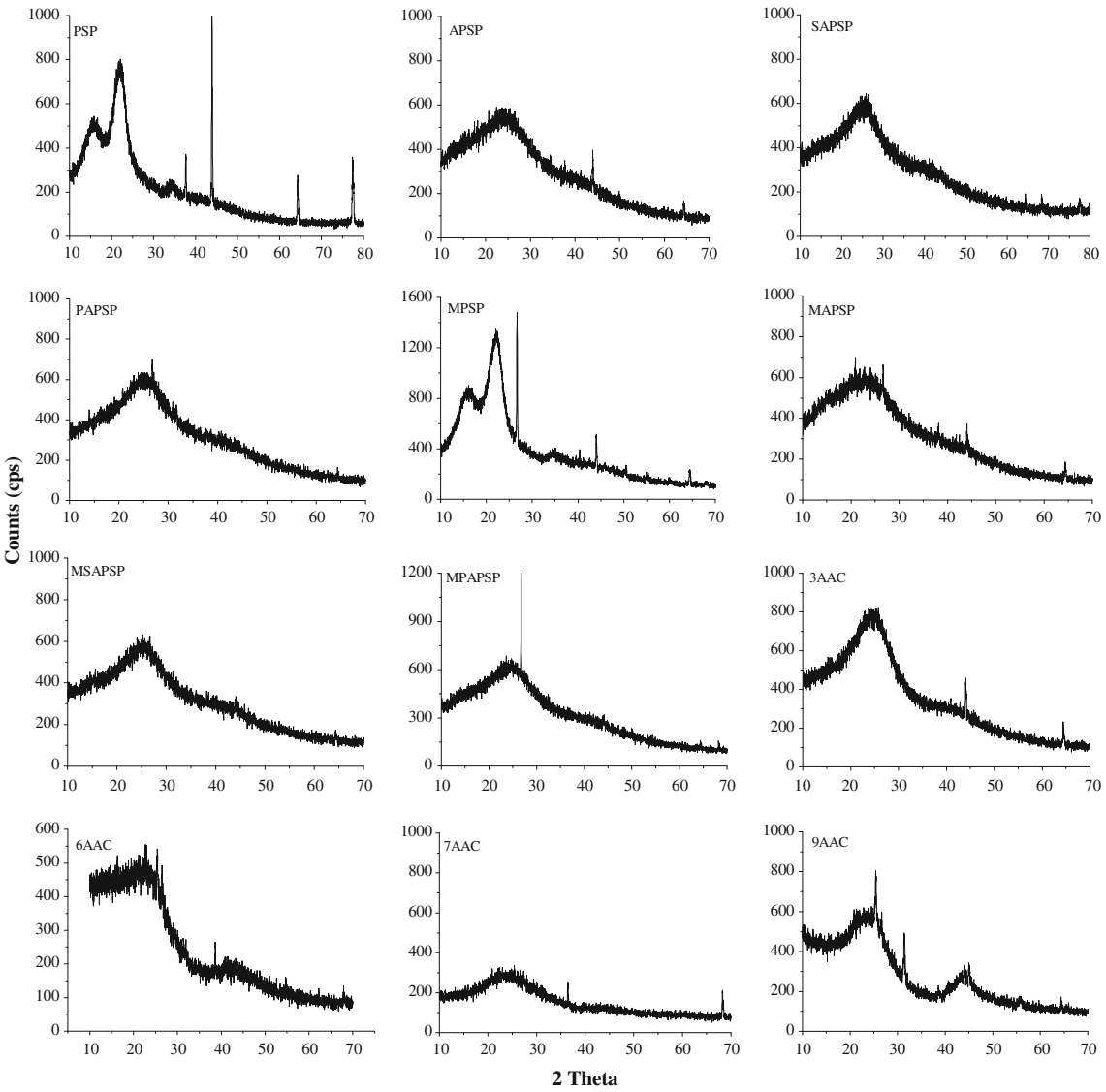

Fig. 4 X-ray diffraction analysis

assigned to out-of-plane deformation vibrations of C–H groups located at the edges of aromatic planes [55–62, 65].

The changes observed in FTIR spectra of APSP at 300, 600, 700 and 900 °C are an evidence for the formation of structures containing multiple carbon–carbon bonds as well as the elimination of originally present hydrogen and oxygen atom. The frequencies between 3,200 and 3,500 cm^{-1} may contain stretching of both amine ($–NH_2$) and alcoholic groups (–OH) which disappears on activation to 300 °C and higher temperatures suggesting dehydration of cellulosic and ligneous components. Lignin substances in APSP, SAPSP and PAPSP show strong absorption (1,510, 1,460 and 1,379 cm^{-1}) till a temperature of 300 °C. As the activation temperature increases from 140 to 300 to 900 °C, the peak around 1,600 cm^{-1} disappears showing the absence of carboxylic acid group as activation temperature increases. A similar phenomenon is seen after acid, persulphate and steam treatment. The peak intensity of –O–H, –C=O and –C–H becomes weak or disappear with the increase of activation temperature of APSP. The results prove that the structure of activated carbons (6AAC, 7AAC and 9AAC) becomes stable due to the decomposition of functional groups with increasing activation temperature (Table 6).

From the above studies it is evident that iodine value is highest for 9AAC followed by 7AAC, 6AAC and 3AAC. MAPSP, MSAPSP and MPAPSP showed slight increase in iodine value, surface area and ion exchange capacity in comparison to APSP, SAPSP and PAPSP respectively. Preliminary studies on the adsorption of Cu, Cd, Zn and Hg on all the adsorbents prepared revealed that MAPSP, MSAPSP, MPAPSP, 3AAC, 6AAC and 7AAC were not

Table 5 FTIR analysis

Sample	PSP	APSP	SAPSP	PAPSP	Intensity	Assignment
Wave numbers (cm^{-1})	3,422.37	3,419.42	3,406.55	3,423.17	Strong	N–H and OH stretching
	1,739.43	–	–	–	Strong	Lactones and 5-membered rings
	1,622.64, 1,510.19, 1,460.53	1,625.29	1,618.12	1,637.52	Variable	C=O, N–H bending
	1,379.06, 1,250.52	1,378.58	1,375.79	1,374.7	Variable	C–O, C–H bending
Sample	MPSP	MAPSP	MSAPSP	MPAPSP	Intensity	Assignment
Wave numbers (cm^{-1})	3,426.55	3,403.92	3,440.59	3,413.44	Strong	N–H and OH stretching
	1,735.04	–	–	–	Strong	Lactones and 5-membered rings
	1,628.46, 1,512.87	1,601.83	1,588.72	1,617.35	Variable	C=O, N–H bending
	1,381.2	–	–	–	Variable	C–O, C–H bending
Sample	3AAC	6AAC	7AAC	9AAC	Intensity	Assignment
Wave numbers (cm^{-1})	2,361.41	–	–	–	Strong	C–H stretching
	1,592.56	–	–	–	Variable	C=O, N–H bending
	1,180.32	–	–	–	Variable	C–O, C–H bending

Table 6 Comparison of adsorbents

Raw material	Carbonisation conditions (°C/h)	Activation conditions (°C/h)	Chemical treatment	BET surface area (m^2/g)	References
Grape seeds	800/1 h (15 °C/min)	800/1 h	Steam activation, one step pyrolysis/activation	497	[5]
Nut shells	800/1 h (15 °C/min)	800/1 h	Steam activation, one step pyrolysis/activation	743	[5]
Pistachio-nut shells	500/2 h (10 °C/min)	900/30 min (10 °C/min)	Physical activation, CO_2	778	[17]
Macadamia nut shells	1 h	500 °C	Chemical activation with both $ZnCl_2$ and KOH	1,718	[18]
Peanut hulls	500/2 h	700–900 °C	Physical activation, two step	81–97, 420	[16]
Almond shells	800/1 h (15 °C/min)	800/1 h	Steam activation, One step pyrolysis/activation	998	[5]
Oat hulls	500 °C/(1.5 s residence)	800/30 min	Steam activation	625	[3]
Cotton stalk	400–700 °C with 7 °C/min	–	–	3, 37	[1]
Oak	700–800 °C	–	Residence time 1–2 h	985	[15]
Corn hulls	700–800 °C	–	Residence time 1–2 h	1,010	[15]
Corn Stover	700–800 °C	–	Residence time 1–2 h	660	[15]
Olive seed	800/1 h	800–900 °C	Residence time 1–2 h, chemical activation, KOH	1,550	[27]
Rice straw	700–1,000/1 h (10 °C/min)	900 °C	Chemical activation, KOH, two step method	2,410	[26]
Rice husk	–	600 °C/3 h	Chemical activation, one step, $ZnCl_2/CO_2$	480	[25]
Pecan shell	–	–	Chemical activation, H_3PO_4	724	[20]
Cassava peel	650/3 h	750 °C	Chemical activation, KOH	1,183	[28]

showing encouraging results (results not shown). We thus decided to restrict to the use of PSP, APSP, SAPSP, PAPSP, MPSP and 9AAC as adsorbents in our further studies. From FTIR spectra it is evident that carboxyl, ether, alcoholic, hydroxyl and amino functional groups may be available for metal binding in PSP, MPSP, APSP, PAPSP and SAPSP while in 9AAC it could be mainly carboxyl groups which are available.

3.7 Selectivity coefficient

The effectiveness of the removal of each metal ion is reflected in the percentage adsorption and selectivity coefficient as reported in Figs. 5, 6, 7 and Table 7 respectively, Adsorption mechanism is as presented in Fig. 8. The selectivity coefficient k was calculated using the equation [66, 67]:

$$k = \frac{\text{molar fraction of component } i \text{ in the carbon adsorbed mixture}}{\text{molar fraction of component } i \text{ in the aqueous solution mixture}} = \frac{q_i/(q_i + q_j)}{CL_i/(CL_i + CL_j)}$$

In quaternary mixtures PAPSP, APSP, SAPSP, 9AAC and MPSP showed higher selectivity towards zinc while PSP showed greater preference towards mercury followed by zinc. SAPSP and PAPSP showed their next preference to copper followed by mercury while APSP, 9AAC and MPSP showed their next preference to mercury over copper.

In ternary mixtures containing Cu, Cd and Hg where zinc was absent all the adsorbents under study showed higher selectivity towards mercury except for SAPSP which showed preference to copper over mercury as also seen in quaternary mixtures. Even in solutions containing Hg, Zn and Cu PSP, MPSP and APSP showed selectivity towards mercury. However, PAPSP and 9AAC again showed better selectivity towards zinc followed by mercury. SAPSP showed selectivity towards copper followed by mercury and zinc. Between copper and cadmium no specific trend was observed with some adsorbents showing selectivity towards copper (PSP, APSP, MPSP) and some towards cadmium (PAPSP) after Hg and Zn.

In binary mixtures of copper and mercury greater selectivity towards mercury was observed by PSP, PAPSP, 9AAC and MPSP. PAPSP showed five times higher selectivity for mercury over copper. On the other hand APSP and SAPSP showed better selectivity towards copper.

Adsorption studies on binary mixtures containing Cd and Hg revealed that all the adsorbents under study showed higher selectivity towards mercury as compared to Cd. Similar studies on binary mixtures containing Zn and Hg revealed that all the adsorbents were selective towards Zn over mercury. However MPSP had almost equal selectivity coefficient values for Zn and Hg.

In binary mixtures containing Cu and Cd, the selectivity coefficients were higher for Cu than Cd in the case of APSP, SAPSP, PAPSP and 9AAC while PSP and MPSP had greater selectivity coefficient values for Cd. APSP, SAPSP, PAPSP and 9AAC displayed higher selectivity towards copper in binary mixtures containing Cu and Zn while PSP and MPSP showed greater selectivity towards zinc. On the other hand, in binary mixtures containing Cd and Zn, PSP, 9AAC, APSP and MPSP showed higher selectivity coefficient for Cd while SAPSP, PAPSP had higher selectivity coefficient for Zn.

In summary, SAPSP seems to show a clear preference for copper except in quaternary mixtures where Zn has a

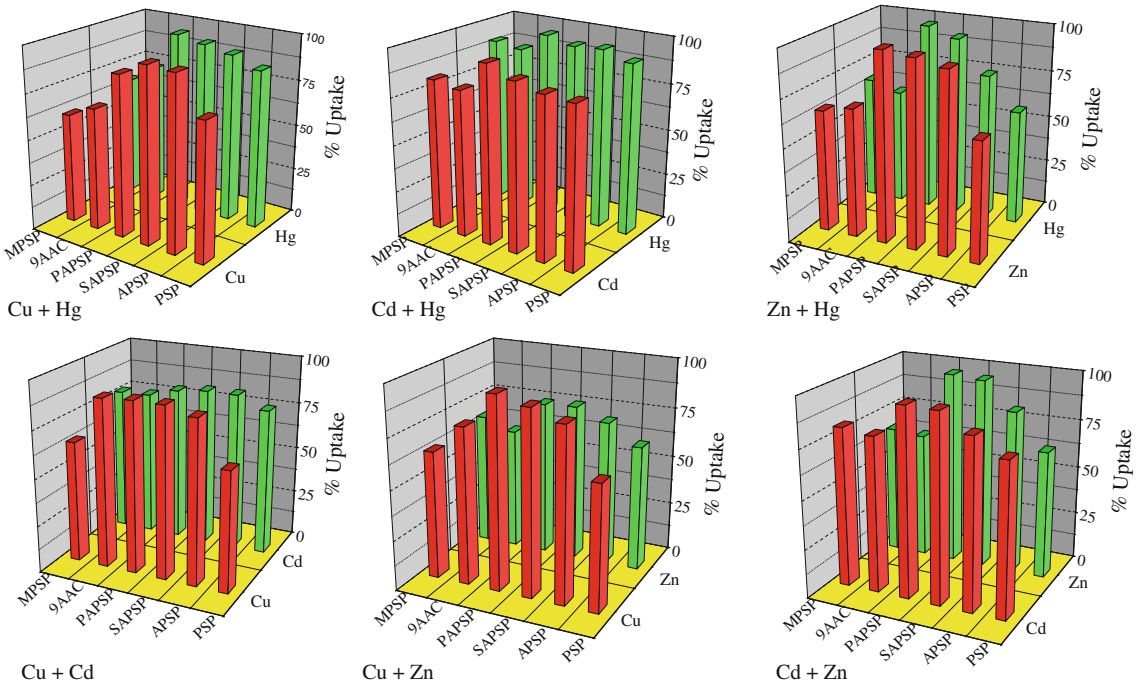

Fig. 5 % Uptake for binary mixtures

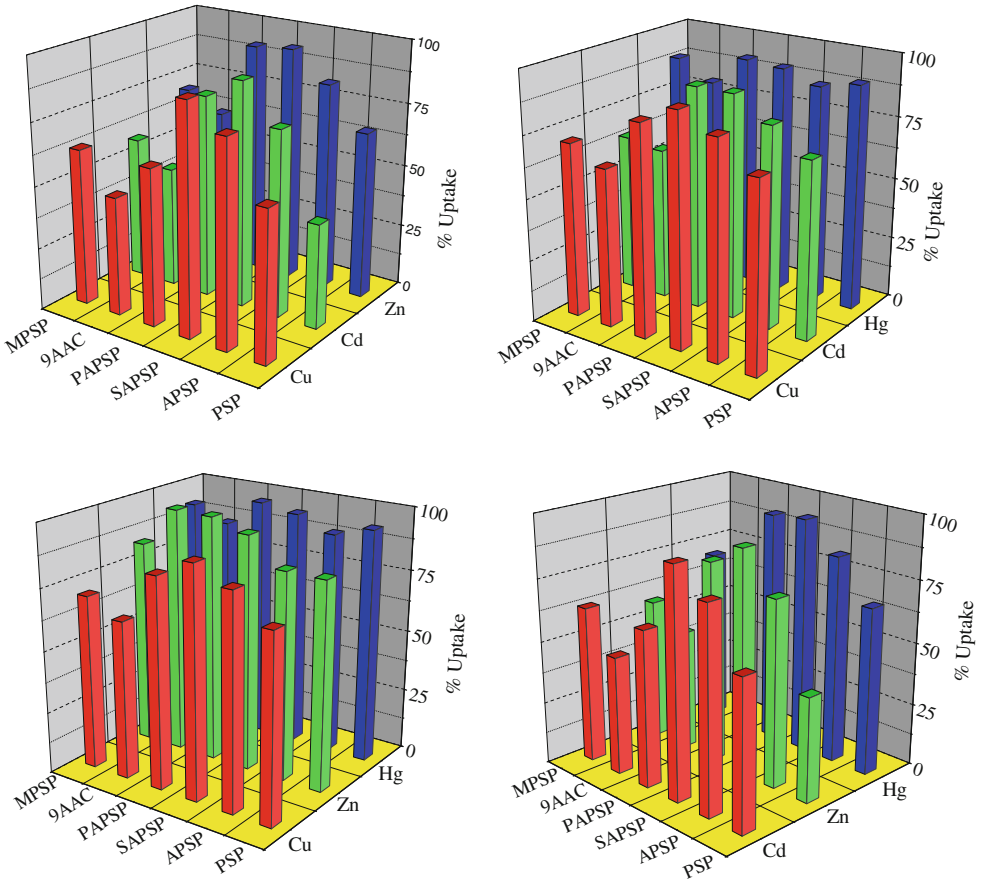

Fig. 6 % Uptake for ternary mixtures

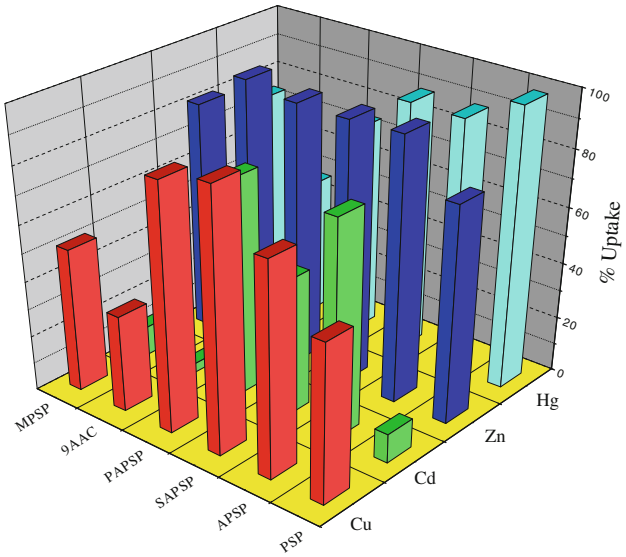

Fig. 7 % Uptake for quaternary mixtures

slightly higher selectivity coefficient, however the difference is very less. PSP on the other hand displayed a greater selectivity towards mercury except for binary mixtures. In binary mixtures probably where individual metal concentrations are higher though the total metal ion concentration continues to be the same PSP showed a different trend by displaying greater selectivity towards Cd in the presence of Cu and Zn, a greater selectivity towards mercury in the presence of Cd and Cu and a greater selectivity towards

Zn in Hg-Zn mixtures. PAPSP showed a clear preference to Zn in quaternary and ternary mixtures and in Cd-Zn and Hg-Zn binary mixtures. Surprisingly, PAPSP showed six times higher selectivity coefficient for copper over Zn in their binary mixtures. MPSP seems to show a clear preference towards mercury in binary and ternary mixtures. However in quaternary mixtures it showed preference towards Zn. APSP and 9AAC did not show any specific trend in the present studies with its selectivity coefficients changing in quaternary, ternary and binary mixtures. This variation in specificity could be because the binding strength of a metal ion to a given adsorbent depends on various properties of the adsorbent and the adsorbate namely ionic radius, hydrolysis constant and electro-negativity of the adsorbate as well as the functional groups and porosity of the adsorbent. It also depends on multiple mechanisms involved in adsorption like ion exchange, chemisorptions, physisorption, dipole interactions, intra-particle diffusion,

Table 7 Selectivity of mixtures

	Cu + Hg		Cd + Hg		Zn + Hg		Cu + Cd		Cu + Zn		Cd + Zn	
	Cu	Hg	Cd	Hg	Zn	Hg	Cu	Cd	Cu	Zn	Cd	Zn
Binary mixtures												
PSP	0.720	1.508	0.748	1.452	1.054	0.948	0.721	1.457	0.993	1.006	1.377	0.755
APSP	1.297	0.808	0.607	2.368	2.816	0.559	1.106	0.910	1.647	0.681	1.118	0.901
SAPSP	1.125	0.898	0.710	1.621	1.672	0.706	1.372	0.774	1.958	0.635	0.777	1.388
PAPSP	0.576	2.978	0.652	2.055	1.019	0.981	1.490	0.734	3.378	0.535	0.669	1.925
9AAC	0.809	1.261	0.731	1.487	1.161	0.866	1.648	0.688	1.567	0.683	1.485	0.714
MPSP	0.878	1.143	0.719	1.540	0.965	1.036	0.743	1.401	0.944	1.060	1.535	0.701

	Cu + Cd + Zn			Cu + Cd + Hg			Hg + Zn + Cu			Hg + Zn + Cd		
	Cu	Cd	Zn	Cu	Cd	Hg	Hg	Zn	Cu	Hg	Zn	Cd
Ternary mixtures												
PSP	1.144	0.563	1.591	0.787	0.662	2.644	2.385	0.755	0.751	15.966	0.957	0.495
APSP	1.107	0.749	1.257	1.069	0.771	1.266	1.299	0.761	1.066	6.724	1.055	0.481
SAPSP	0.923	0.799	1.467	1.118	0.840	1.086	1.029	0.904	1.081	11.567	2.988	0.359
PAPSP	0.450	1.150	3.450	0.666	1.076	1.627	0.938	1.957	0.697	8.531	2.901	0.373
9AAC	0.808	0.842	1.482	0.799	0.725	1.938	0.889	12.807	0.492	1.590	12.857	0.366
MPSP	0.980	0.777	1.338	0.823	0.608	2.714	1.730	0.736	0.903	9.669	1.772	0.353

	Cu + Cd + Zn + Hg			
	Cu	Cd	Zn	Hg
Quaternary mixtures				
PSP	1.38E−02	2.95E−03	0.033	0.960
APSP	0.059	0.065	0.271	0.155
SAPSP	0.188	1.78E−02	0.203	0.133
PAPSP	0.124	0.063	0.227	0.055
9AAC	5.96E−03	1.91E−03	0.172	9.33E−03
MPSP	1.09E−02	2.75E−03	0.041	0.027

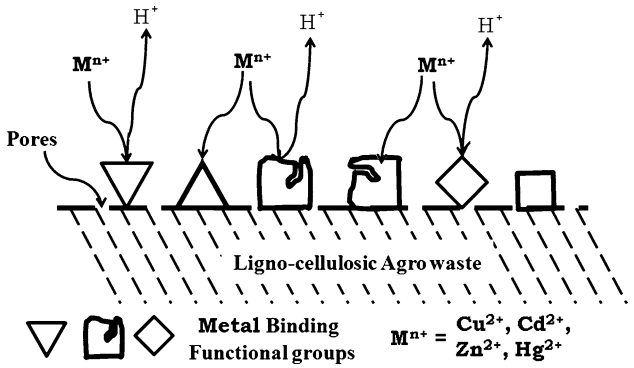

Fig. 8 Mechanism of adsorption

pore diffusion etc. However, it is observed that mercury and zinc showed quantitative adsorption (>90%) in binary, ternary and quaternary mixtures with most of the adsorbents under study. Thus further studies using different concentrations and adsorption models are definitely warranted to get a clear picture of the selectivity.

4 Conclusions

A series of adsorbents were prepared from sulfuric acid treated PSP by steam, persulfate and formaldehyde treatment at 140 °C and acid treatment followed by carbonization at different temperatures. The adsorbents were characterized using SEM, FTIR, TGA and XRD. Protonation and polymerization of PSP, APSP, SAPSP and PAPSP by formaldehyde solution prevented leaching from the biomass though there was no large increase in surface area. In the case of APSP there was not much change in pore volume as compared to PSP but pore diameter increased from 237.984 Å for PSP to 422.65 Å for APSP. It was found that persulphate treatment gives rise to decrease in

surface area, destruction and widening of the micro-pores (9,829.99 Å) and an increase in pore volume (0.022 cm^3/g). While in the case of SAPSP there was not much change in pore volume but pore diameter decreased from 237.984 to 81.244 Å. Interestingly APSP, SAPSP and PAPSP were found to have iodine values of 342.5, 199.8 and 299.7 respectively and significant pore size in spite of their small BET surface areas suggesting high sorption capacity. The activated carbon 9AAC had maximum surface area of 834 m^2/g and pore volume 0.4474 cm^3/g as well as high iodine value. FTIR spectral data indicate that carboxyl, ether, alcoholic, hydroxyl and amino functional groups may be available for metal binding in PSP, MPSP, APSP, PAPSP and SAPSP while in 9AAC it could be mainly carboxyl groups which are available. Therefore, from a practical point of view, by carefully applying relevant modification techniques, it is possible to prepare adsorbents for specific environmental applications. Selectivity coefficients for different mixtures containing mercury, copper, zinc and cadmium have been determined for PSP, MPSP, APSP, SAPSP, PAPSP and 9AAC. Though PSP, APSP, SAPSP, PAPSP and MPSP did not have appreciable surface area, they showed encouraging results for adsorption of heavy metals indicating the potential use of palm shell as an economic precursor in the activated carbon preparation process. These preliminary results warrant further investigations. We are currently engaged in further studies to apply this range of new adsorbents for the removal of trace metal ions and gain insight into the adsorption mechanism.

Acknowledgments This work has been funded by the Board of research in Nuclear Sciences, INDIA. The authors also thank Dr. P. K. Mehta, Department of Physics, for the XRD analysis and Dr. V. J. Rao, Department of Metallurgy and Material Science, for TGA and SEM analysis, The M. S. University of Baroda and Head Department of Chemistry, The M. S. University of Baroda, for Laboratory facilities.

References

1. F.R. Reinoso, M.M. Sabio, Carbon **30**, 1111–1118 (1992)
2. A.A. El-Hendawy, Carbon **41**, 713–722 (2003)
3. R.M. Suzuki, A.D. Andrade, J.C. Sousa, M.C. Rollemberg, Biores. Technol. **98**, 1985–1991 (2007)
4. A.A. El-Hendawy, A.J. Alexander, R.J. Andrews, G. Forrest, J. Anal. Appl. Pyrolysis **82**, 272–278 (2008)
5. F. Rodriguez-Reinoso, J. Lahaye, P. Ehrburger (eds.), *Fundamental Issue in Control of Carbon Gasification Reactivity* (Kluwer, Dordrecht, 1991), pp. 533–571
6. K. Tomkow, A. Jankowska, F. Chechowsk, T. Siemieniewska, Fuel **56**, 266–270 (1977)
7. C.T. Hsieh, H. Teng, Carbon **38**, 863–869 (2000)
8. I. Martin-Gullon, R. Font, Water Res. **35**, 516–520 (2001)
9. Q. Li, V.L. Snoeyink, B.J. Marinas, C. Campos, Water Res. **37**, 773–784 (2003)
10. K. Nakagawa, A. Namba, S.R. Mukai, H. Tamon, P. Ariyadejwanich, Water Res. **38**, 1791–1798 (2004)
11. Z. Yue, J. Economy, K. Rajagopalan, G. Bordson, M. Piwoni, L. Ding, V.L. Snoeyink, B.J. Marinas, J. Mater. Chem. **16**, 3375–3380 (2006)
12. S. Han, K. Sohn, T. Hyeon, Chem. Mater. **12**, 3337–3341 (2000)
13. H. Tamai, T. Kakii, Y. Hirota, T. Kumamoto, H. Yasuda, Chem. Mater. **8**, 454–462 (1996)
14. A. Oya, S. Yoshida, J. Alcaniz-Monge, A. Linares-Solano, Carbon **33**, 1085–1090 (1995)
15. T. Kyotani, T. Nagai, S. Inoue, A. Tomita, Chem. Mater. **9**, 609–615 (1997)
16. S. Han, T. Hyeon, Chem. Commun. **19**, 1955–1956 (1999)
17. Z. Li, M. Jaroniec, J. Am. Chem. Soc. **123**, 9208–9209 (2001)
18. L. Lee, S. Yoon, S.M. Oh, C. Shin, T. Hyeon, Adv. Mater. **12**, 359–362 (2000)
19. T.A. Kurniawan, G.Y.S. Chan, W. Lo, S. Babel, Sci. Total Environ. **366**, 409–426 (2006)
20. D. Mohan, K.P. Singh, Water Res. **36**, 2304–2318 (2002)
21. M. Kobya, E. Demirbas, E. Senturk, M. Ince, Bioresour. Technol. **96**, 1518–1521 (2005)
22. A. Demirbas, J. Hazard. Mater. **157**, 220–229 (2008)
23. C.K. Singh, J.N. Sahu, K.K. Mahalik, C.R. Mohanty, B.R. Mohan, B.C. Meikap, J. Hazard. Mater. **153**, 221–228 (2008)
24. J. Kim, M. Sohn, D. Kim, S. Sohn, Y. Kwon, J. Hazard. Mater. **85**, 301–315 (2001)
25. H. Demiral, I. Demiral, F. Tümsek, B. Karabacakoglu, Chem. Eng. J. **144**, 188–196 (2008)
26. K. Kadirvelu, M. Kavipriya, C. Karthika, M. Radhika, N. Vennilamani, S. Pattabhi, Bioresour. Technol. **87**, 129–132 (2003)
27. N.A. Khan, S. Ibrahim, P. Subramaniam, Malays. J. Sci. **23**, 43–51 (2004)
28. G. Sreelatha, S. Kushwaha, V.J. Rao, P.P. Sudhakar, Ind. Eng. Chem. Res. **49**, 8106–8113 (2010)
29. S. Kushwaha, G. Sreelatha, P. Padmaja, J. Chem. Eng. Data. doi: 10.1021/je1013334
30. ASTM, *Standard Test Method for Determination of Iodine Number of Activated Carbon* (ASTM Committee on Standards, ASTM, Philadelphia, 2006), pp. 4607–4694
31. A. Aziz, M.S. Ouali, E.H. Elandaloussi, J. Hazard. Mater. **163**, 441–447 (2009)
32. P. Galiatsatou, M. Metaxas, V. Kasselouri-Rigopoulou, J. Hazard. Mater. **B91**, 187–203 (2002)
33. R. Baccar, J. Bouzid, M. Feki, A. Montiel, J. Hazard. Mater. **162**, 1522–1529 (2009)
34. P.R.F. Campos, M.Sc. Dissertation, Departamento de Engenharia Quimica, UEM, 1996, pp. 1–95
35. C. Naizhen, H. Darmstadt, R. Christian, Energy Fuels **15**, 1263–1269 (2001)
36. K. Gergova, N. Petrov, V. Minkova, J. Chem. Technol. Biotechnol. **56**, 77–82 (1993)
37. P.A. Bazuła, A.H. Lu, J.J. Nitz, F. Schuth, Microporous Mesoporous Mater. **108**, 266–275 (2008)
38. K. Gergova, N. Petrov, S. Eser, Carbon **32**, 693–702 (1994)
39. L. Krisztina, B. Attila, G.N. Lajos, Carbon **38**, 1965–1976 (2000)
40. J.P. Fraissard, *Physical Adsorption: Experiment, Theory, and Applications*, NATO ASI Series (Kluwer, Dordrecht, 1996), pp. 9–17
41. F.R. Reinoso, A.L. Solano, in *Chemistry and Physics of Carbon*, vol. 21, ed. by P.A. Thrower (Marcel Dekker, New York, 1989), pp. 1–146
42. S.J. Gregg, K.S.W. Singh, *Adsorption Surface Area and Porosity* (Academic Press, New York, 1982), pp. 303–305
43. T. Ohba, K. Kaneko, Langmuir **17**, 3666–3670 (2001)
44. M.J. Remy, G. Poncelet, J. Phys. Chem. **99**, 773–779 (1995)
45. D. Adinata, M.A.W.D. Wan, M.K. Aroua, Biores. Technol. **98**, 145–149 (2007)

46. S. Ismadji, S.K. Bhatia, Langmuir **16**, 9303–9313 (2000)
47. S. Ismadji, S.K. Bhatia, Langmuir **17**, 1488–1498 (2001)
48. P.T. Williams, A.R. Reed, J. Anal. Appl. Pyrolysis **70**, 563–577 (2003)
49. F. Stoeckli, A. Guillot, A.M. Slasli, D. Hugi-Cleary, Carbon **40**, 211–215 (2002)
50. M. Koyama, W. Helbert, T. Imai, J. Sugiyama, B. Henrissat, Proc. Natl. Acad. Sci. USA **94**, 9091–9095 (1997)
51. K. Marco, S.N. Peter, G.J. Mark, K. Markus, Environ. Sci. Technol. **44**, 1247–1253 (2010)
52. W. Huang, H. Zhang, Y. Huang, W. Wang, S. Wei, Carbon **49**, 838–843 (2011)
53. A.K. Kercher, D.C. Nagle, Carbon **41**, 15–27 (2003)
54. O. Paris, C. Zollfrank, G.A. Zickler, Carbon **43**, 53–67 (2005)
55. B.J. Meldrum, C.H. Rochester, J. Chem. Soc. Faraday Trans. **86**, 1881–1884 (1990)
56. B.J. Meldrum, C.H. Rochester, J. Chem. Soc. Faraday Trans. **86**, 861–865 (1990)
57. G. Socrates, *Infrared Characteristic Group Frequencies*, 2nd edn. (Wiley, Chichester, 1994), pp. 50–94
58. P.E. Fanning, M.A. Vannice, Carbon **31**, 721–730 (1993)
59. B.J. Meldrum, C.H. Rochester, J. Chem. Soc. Faraday Trans. **86**, 2997–3002 (1990)
60. B.J. Meldrum, C.H. Rochester, J. Chem. Soc. Faraday Trans. **86**, 3647–3652 (1990)
61. M. Nakahara, S. Asai, Y. Sanada, T. Ueda, J. Mater. Sci. **30**, 5667–5671 (1995)
62. M. Nakahara, Y. Sanada, J. Mater. Sci. **30**, 4363–4365 (1995)
63. J. Zawadzki, in *Chemistry and Physics of Carbon*, vol. 21, ed. by P.A. Thrower (Marcel Dekker, New York, 1989), pp. 147–380
64. L. Dupont, E. Guillon, Environ. Sci. Technol. **37**, 4235–4241 (2003)
65. S. Biniak, G. Szymanski, J. Siedlewski, A. Swiatkowski, Carbon **35**, 1799–1810 (1997)
66. F. Stoeckli, M.V. Lopez-Ramon, D. Hugi-Cleary, A. Guillot, Carbon **39**, 1115–1116 (2001)
67. A.R. Khan, I.R. Al-Waheab, A. Al-Haddad, Environ. Technol. **17**, 13–23 (1996)